

# Precision Dilution in Triangulation Based Mobile Robot Position Estimation

Alonzo KELLY

*Robotics Institute*

*Carnegie Mellon University*

*Pittsburgh, PA 15213-3890*

*email: alonzo@rec.ri.cmu.edu*

**Abstract.** When navigating from landmarks, the numerical computation of the differential behavior of the mapping from measurements to states is well understood. This paper seeks to develop tools to foster an intuitive grasp of the spatial variation in the differential behavior of this mapping. Graphical methods are adapted from marine navigation in order to introduce the issues in low dimensional cases. The implicit function theorem and the pseudoinverse are then used in the general case to derive a quantity analogous to the geometric dilution of precision (GDOP) as it is used in satellite based guidance. An explicit expression is obtained for the conditioning of the triangulation computation as a function of position. This expression also directly provides the conditions under which the computation becomes singular. The application to a few common cases is illustrated.

## 1. Introduction

The ancient application of techniques for solving triangles to problems in geometry (literally “earth measurement”) and navigation are well documented [16]. Due to a lack of a more general term, the term triangulation is often used today to refer to any process which solves a system of simultaneous algebraic or transcendental equations — whether or not they are reducible to an equivalent problem involving triangles.

In mobile robots, triangulation occurs often in the context of explicit point landmarks, often viewed by a vision system. However, any aspects of the environment whose positions are known, viewed by any sensor whose indications depend on their position relative to the sensor, establishes a triangulation context.

Triangulation differs materially from dead reckoning. In dead reckoning from inertial indications (inertial navigation) [4] or ground referenced velocity indications, errors propagate according to governing differential equations leading to time dependent behavior of localization error. Dead reckoning errors have dynamics — the present state error depends, at any time, on the entire measurement error history.

By contrast, triangulation errors do not exhibit dynamics. The present state error depends, at any time, only on the present measurement error. The first order mapping between them depends, in turn, on the configuration of the landmarks relative to the robot. This paper provides some convenient tools for understanding the behavior of this mapping in a framework which is consistent with an equivalent recent analysis for odometry [7].

The goal of the paper is to develop methods to visualize and analytically compute the gross magnification factor which transforms sensor error magnitudes into computed pose error magnitudes. In satellite navigation systems, this factor is known as the geometric dilu-

tion of precision.

### 1.1 Previous Work

In mobile robotics, an early survey of approaches to position estimation appears in [14]. With the notable exception of [1], there is little direct precedent for analytic computation of the conditioning of triangulation computations. [1] uses a complex number representation of bearing observations of landmarks and computes the conditions for singularity of the pseudoinverse. For example, [2] exemplifies numerical study of triangulation error and it reaches conclusions which are supported by the theory presented here. Likewise, the widespread use of the Kalman filter in mobile robots means that the numerical computation of uncertainty predictions are often a fundamental aspect of system operation. In contrast to such computations, this paper seeks analytic results for their intuitive, pedagogic, and theoretical value.

Early work on localizing from landmarks using sonar appears, for example, in [3] and [10]. For the case of using cameras, [8] extends the work of [13] in addressing the case of using rays (bearings) from a single image. Empirical analysis of the generated pose errors is provided. Analytic results are deemed to be difficult to produce for the case studied. In the case of stereo, [11] is among some of the earliest work which accounts explicitly for stereo uncertainty in a navigation context.

Elsewhere in robotics, the conditioning of the observer Jacobian is the same issue as that of the feature velocity Jacobian computed in visual servoing [6]. This computation considers the mapping from image velocities to scene velocities. Similarly, the conditioning of the mapping from cartesian rates to joint rates is central to resolved rate manipulator control [15].

Outside robotics, the fields of survey and guidance, of course, have studied triangulation and its numerical stability. For the Global Positioning System (GPS) [12], for example, a form of the geometric dilution of precision (GDOP) is often computed explicitly in contemporary signal receivers.

### 1.2 Problem Description

For the present purpose, the formulation of triangulation as an observer process is particularly useful. Let the vehicle position and orientation (pose) be collected into a state vector thus:

$$\underline{x}(t) = [x(t) \ y(t) \ \theta(t)]^T \quad (1)$$

Let  $\underline{z}$  denote a vector of observations (measurements) which are related to the mobile robot state  $\underline{x}$  by a general nonlinear measurement function as follows:

$$\underline{z} = h(\underline{x}) \quad (2)$$

While, in particular cases, the relationship may be linear and while in others the relationship may be invertible in closed form (to determine  $\underline{x}$  as an explicit function of  $\underline{z}$ ), the above observer form is applicable more generally.

One view of the above relationship is that each element of the observation provides a constraint on the state. When sufficient constraints are available, the system can be solved for the robot position. However, it is common in robotics to solve the above system in both underconstrained and overconstrained cases.

The measurements can in principle be any physically observable quantity which is determined by vehicle pose but in practice, observations of range, bearing, or cartesian position of landmarks are common.

This paper addresses the following problem. Let the observations be corrupted by addi-

tive errors  $\delta \underline{z}(t)$  as follows:

$$\underline{z}'(t) = \underline{z}(t) + \delta \underline{z}(t) \quad (3)$$

Using these input errors and the observer relationship, determine the behavior of the associated errors in the computed vehicle pose:

$$\begin{aligned} x'(t) &= x(t) + \delta x(t) \\ y'(t) &= y(t) + \delta y(t) \\ \theta'(t) &= \theta(t) + \delta \theta(t) \end{aligned} \quad (4)$$

The errors can be systematic or random in nature, and solutions for either case are sought.

## 2. Intuitive Concepts

### 2.1 Level Curves of Observation

A particularly useful visualization of triangulation is the level curves, or contours, which emerge when the observer is viewed as a scalar field over pose space. Conceptually, for the single element of the observation vector  $z_i$ , the implicitly defined curve or surface:

$$z_i = h_i(\underline{x}) = \text{constant} \quad (5)$$

is the locus of all points for which the “constraint” is satisfied, or in more familiar terms, the collection of poses which are consistent with the observation. Historically, hand drafting of such “lines of position” was a basic technique in marine navigation from landmarks [5]. In the computer age, numerical techniques to solve systems like Equation (2) by linearization and iteration are well known. The fact that a mobile robot’s position changes very little over the typical time period between observations often means that the typical difficulties of determining a good initial guess can be avoided by simply using the last estimate, possibly augmented by intermediate odometry, as the prior estimate for the current iteration.

For this view, the visualization is particularly effective when the state vector is limited to the two dimensional position of the robot - that is, when  $\underline{x} = [x \ y]^T$ . The balance of the paper assumes that an association has been accomplished between sensor indications and the landmarks to which they correspond.

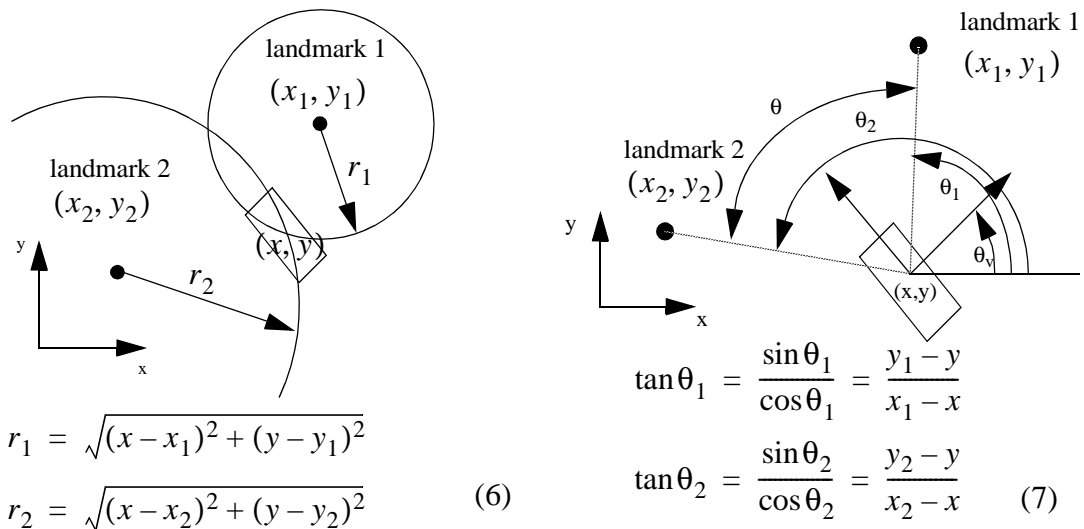


**Figure 1: Lines of Position.** Such diagrams enable the visualization of triangulation as a process of concurrent satisfaction of multiple level curves of constraint. Left: range measurements generate circular constraints. Right: bearing measurements generate linear constraints (although the observer itself is a nonlinear function of the state).

For example, consider the cases shown in Figure 1. Discrete landmarks are observed through a ranging device in the left figure and a bearing indicator in the right figure. The left system is analogous to the GPS satellite guidance system [9]. The right figure is analogous to both laser guidance of contemporary autonomous guided vehicles and camera based guidance used more commonly in research laboratories. In either case, it is clear that the robot position must be a point where both constraints are satisfied (where the circles or lines intersect). In some cases, this point is not necessarily unique and in others it does not exist. There is no solution when the circles do not intersect, when the lines are parallel, or when the robot is over a landmark. Generally, nonlinear constraints lead to a set of issues concerning existence and uniqueness of solutions and the conditioning of computations when the two solutions are near each other.

## 2.2 First Order Response to Perturbations

Error propagation can be understood in this intuitive framework by imagining how small variations in the observations will impact the computed solution for vehicle position. On contour diagrams, the volume enclosed by original and perturbed level curves is, by construction, the region which is generated by the associated perturbations to the observations. Figure 2, illustrates how these volumes can be constructed graphically. Both the volume and the shape of the region are meaningful.

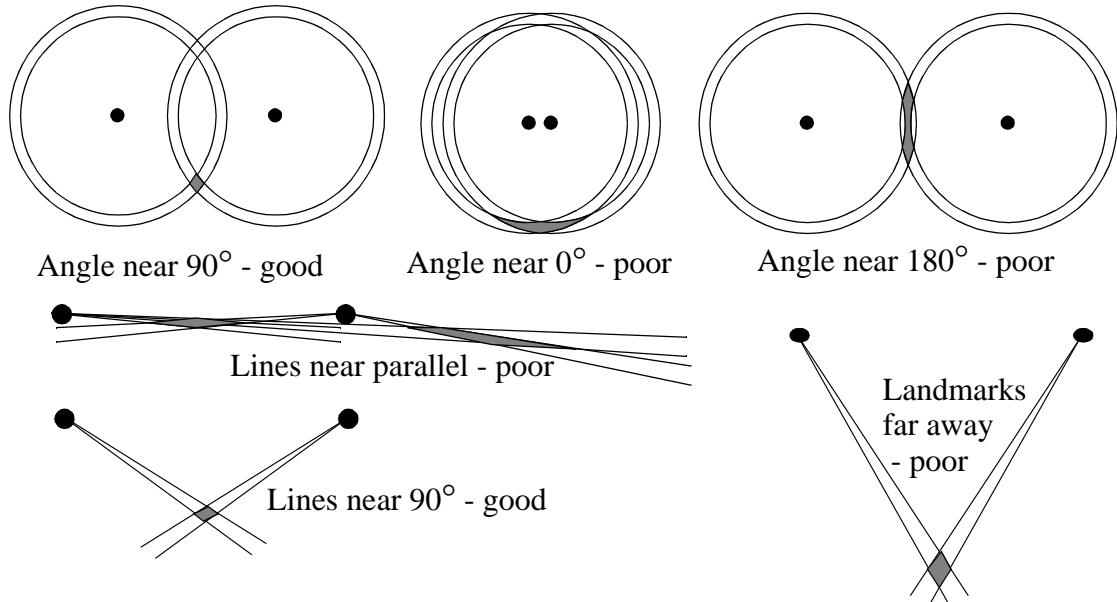


**Figure 2: Error Regions and Sensitivity.** The shaded region is spanned by the computed pose in response to perturbations in the observations. For a fixed error input, the region's size and the shape changes as the robot moves with respect to the landmarks

A final important aspect of error propagation is the dependence of the differential behavior on the state (the pose of the robot). This dependence again derives fundamentally from the nonlinear nature of the observer.

All of these issues come to light when a region is entirely filled with contours whose levels are equally spaced as shown in Figure 3.

## 3. Analytical Concepts

In more general, higher dimensional cases, a two dimensional contour view is not as illuminating and intuition must give way to more formal methods.

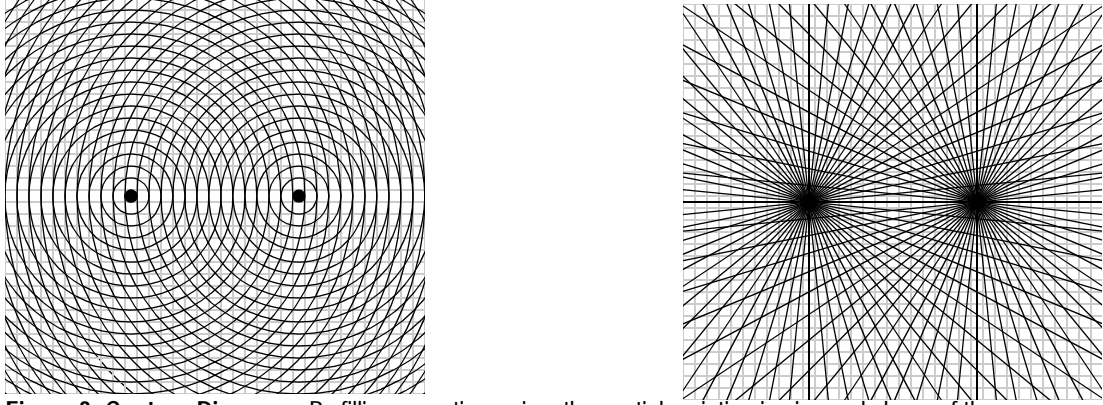


**Figure 3: Contour Diagrams.** By filling an entire region, the spatial variation in size and shape of the response to an unit input error can be visualized at once.

### 3.1 First Order Response to Perturbations

Clearly, the first order behavior of the observer is straightforward. If  $H = \partial h / \partial x$  is the Jacobian of the observer, then systematic and random errors in the observations are related to corresponding errors in the states by

$$\delta \underline{z} = H \delta \underline{x} \qquad C_{\underline{z}} = H C_{\underline{x}} H^T \quad (8)$$

where  $C_{\underline{z}}$  is the measurement covariance and  $C_{\underline{x}}$  is the associated state covariance (when the errors are interpreted as random variables). They are defined as:

$$C_{\underline{z}} = \text{Exp}[\delta \underline{z} \delta \underline{z}^T] \qquad C_{\underline{x}} = \text{Exp}[\delta \underline{x} \delta \underline{x}^T] \quad (9)$$

In practice,  $\delta \underline{z}$  is more likely to be considered known and  $\delta \underline{x}$  is to be determined, so the above differential relationships usually need to be inverted:

$$\delta \underline{x} = H^+ \delta \underline{z} \qquad C_{\underline{x}} = (H^T C_{\underline{z}}^{-1} H)^{-1} \quad (10)$$

where the superscript “+” denotes the pseudoinverse. From a numerical perspective, Equation (10) can be considered to be the solution to the linearized error transformation problem for both the systematic and stochastic case. However, we seek an economical analytic expression for the conditioning of this mapping.

### 3.2 Jacobian Determinant as GDOP

We are normally interested in the magnification from the perspective of how sensor errors are magnified to become pose errors. Let us loosely define the geometric dilution of precision, or GDOP, as:

$$GDOP = \|\delta \underline{x}\| / \|\delta \underline{z}\| \quad (11)$$

where  $\|\delta \underline{x}\|$  and  $\|\delta \underline{z}\|$  are the “magnitudes” of pose and sensor errors respectively according to any useful definition of magnitude.

Clearly, the mapping between sensor error and pose error is a matrix and any sort of norm of the matrix is a measure of the relative magnifying power of the matrix. Among the choices of norm available, the Jacobian determinant is a convenient choice because it avoids eigenvalue computations. When the observer system is square, the Jacobian determinant expresses the scalar multiplier which converts a differential volume in pose space to its cor-

responding differential volume in measurement space:

$$\|\delta_{\underline{z}}\| = \|H\|\|\delta_{\underline{x}}\| \quad \|\delta_{\underline{x}}\| = \|H^{-1}\|\|\delta_{\underline{z}}\| = \frac{1}{\|H\|}\|\delta_{\underline{z}}\| \quad (12)$$

Where the volumes are  $\|\delta_{\underline{x}}\| = \delta x_1 \delta x_2 \delta x_3$  and  $\|\delta_{\underline{z}}\| = \delta z_1 \delta z_2 \delta z_3$  and  $DOP = \|H^{-1}\|$  the determinant of the inverse Jacobian. The  $\|\ \|$  notation is intended to represent both the volume of a vector and determinant of a matrix since these are consistently related by Equation (12).

In the more general case, the measurements are only implicit functions of the states and we have:

$$f(\underline{x}, \underline{z}) = \underline{0} \quad (13)$$

and by taking the total differential:

$$[f_z]\delta_{\underline{z}} = -[f_x]\delta_{\underline{x}} \quad (14)$$

where  $f_z = \partial f / \partial z$  and  $f_x = \partial f / \partial x$ . This system can be solved in either direction by the pseudoinverse:

$$\delta_{\underline{z}} = -[f_z]^+ [f_x] \delta_{\underline{x}} \quad \delta_{\underline{x}} = -[f_x]^+ [f_z] \delta_{\underline{z}} \quad (15)$$

and Equation (12) then applies.

When the system is fully determined, both Jacobians are square. Using the rules for the determinant of a product and the determinant of a matrix inverse, we have:

$$\|H\| = \|f_x\| / \|f_z\| \quad (16)$$

This form will be useful for the following examples.

## 4. Results

Two cases can be illustrated in the available space.

### 4.1 Circular Constraints

Consider the case of navigating from range indications of known point landmarks. In this case, the constraint equations are circles as shown in Equation (6). Equation (8) becomes:

$$\begin{bmatrix} dr_1 \\ dr_2 \end{bmatrix} = \begin{bmatrix} \frac{x-x_1}{r_1} & \frac{y-y_1}{r_1} \\ \frac{x-x_2}{r_2} & \frac{y-y_2}{r_2} \end{bmatrix} \begin{bmatrix} dx \\ dy \end{bmatrix} \quad (17)$$

By reference to Figure 4 this determinant can be shown (through vector algebra) to be equivalent to the cosecant of the relative bearing angle between the two landmarks.

$$\begin{aligned} \|H\| &= \begin{pmatrix} \frac{x-x_1}{r_1} & \frac{y-y_1}{r_1} \\ \frac{x-x_2}{r_2} & \frac{y-y_2}{r_2} \end{pmatrix} - \begin{pmatrix} \frac{y-y_1}{r_1} & \frac{x-x_2}{r_2} \end{pmatrix} \\ \|H\| &= \frac{\vec{r}_1 \times \vec{r}_2}{\|\vec{r}_1\| \|\vec{r}_2\|} = \sin(\theta) \\ \|H^{-1}\| &= \frac{1}{\sin(\theta)} \end{aligned}$$

**Figure 4: GDOP for Circular Constraints.** The GDOP is the cosecant of the relative bearing angle between the two landmarks.

Heading cannot be determined from ranges to a single point on the robot, so it was removed from the state vector. Clearly, the GDOP tends to infinity when either the robot is on the line between the landmarks (when the position orthogonal to the line between them becomes unconstrained) or when it is so far away that the position parallel to the line between them becomes unconstrained. The GDOP is best when the angle between the landmarks is a right angle. All of these cases were predicted in Figure 2.

#### 4.2 Linear Constraints

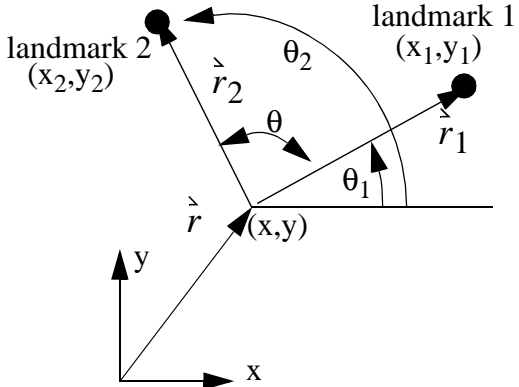
Consider the case of navigating from bearing indications of known point landmarks with known heading. In this case, the constraint equations are lines as shown in Equation (7). Equation (13) takes the form:

$$\begin{aligned} s_1(x_1 - x) - c_1(y_1 - y) &= s_1\Delta x_1 - c_1\Delta y_1 = 0 \\ s_2(x_2 - x) - c_2(y_2 - y) &= s_2\Delta x_2 - c_2\Delta y_2 = 0 \end{aligned} \quad (18)$$

where  $\Delta x_1 = x_1 - x$  etc. and  $s_1 = \sin(\theta_1)$  etc. Equation (16) is, in this case:

$$\|H\| = \frac{\|f_x\|}{\|f_z\|} = \left\| \begin{array}{c} -s_1 \ c_1 \\ -s_2 \ c_2 \end{array} \right\| \left\| \begin{array}{cc} c_1\Delta x_1 + s_1\Delta y_1 & 0 \\ 0 & c_2\Delta x_2 + s_2\Delta y_2 \end{array} \right\| \quad (19)$$

By reference to Figure 5 this determinant can be shown (through vector algebra) to be equivalent to the product of the range product and the cosecant of the relative bearing angle between the two landmarks.

$$\begin{aligned} \|H^{-1}\| &= \left( \frac{\vec{r}_1 \cdot \vec{r}_1}{|\vec{r}_1|} \cdot \frac{\vec{r}_2 \cdot \vec{r}_2}{|\vec{r}_2|} \right) / \frac{|\vec{r}_1 \times \vec{r}_2|}{|\vec{r}_1||\vec{r}_2|} \\ \|H^{-1}\| &= \frac{r_1 r_2}{\sin(\theta)} \end{aligned}$$


**Figure 5: GDOP for Linear Constraints.** The GDOP is the range product times the cosecant of the relative bearing angle between the two landmarks.

For this case, the GDOP again tends to infinity when the robot is on the line between the landmarks. As the range product becomes large, the angle between the sight lines also becomes small and the conditioning degrades quickly. The GDOP is best when the angle between the landmarks is a right angle and the landmarks are close. All of these cases were predicted in Figure 2.

## 5. Conclusions

While the mapping from sensor errors to pose errors in triangulation is a straightforward numerical computation (based on linearizing the observation equations), such solutions generate little insight into the underlying mechanisms or the general case. While contour diagrams are intuitively appealing, they do not scale well to higher dimensions. An analytical technique has been introduced which produces in closed-form an expression for the scaling

volumes in sensor error space into volumes in pose error space. This expression also produces the conditions under which triangulation becomes ill-conditioned.

Such analytic expressions are catalysts for the development of theory. They can be substituted into other closed-form analyses or differentiated in optimization processes. For example, the “optimal” configuration of landmarks can be computed from the above results as the one for which GDOP is best overall for a given work envelope. It is possible to show that direct observation of range differences, a marine radio-navigation technique known as hyperbolic navigation, is exceptionally well-behaved.

For pedagogic purposes, these results amount to a process for proof of the conditions under which computation becomes ill conditioned. Rules of thumb are produced which are valuable design heuristics. They form the basis of requirements analysis which, for example, requires a third landmark in order to determine heading or disambiguate multiple solutions in many cases.

## 6. References

- [1] M Betke and L. Gurvits, “Mobile Robot Localization Using Landmarks”, IEEE Transactions on Robotics and Automation, Vol. 13, No. 2, April 1997.
- [2] C. Cohen and F. Koss, “A Comprehensive Study of Three Object Triangulation”, Proceedings of the 1993 SPIE Conference on Mobile Robots, Boston, Ma., Nov 18-20 1993.
- [3] J. L. Crowley, "Navigation for an Intelligent Mobile Robot", IEEE Journal on Robotics and Automation, JRA 1 (1), March 1985.
- [4] M. Fernandez, and G. R. Macomber G. R., “Inertial Guidance Engineering”, Prentice Hall, Englewood Cliffs, NJ, 1962.
- [5] R. Hobbs, “Marine Navigation. Piloting and Celestial and Electronic Navigation.” Third Edition, Naval Institute Press, Annapolis, Maryland. 1990.
- [6] S. Hutchinson, G. Hager, P. Corke, “A Tutorial on Visual Servo Control”, IEEE Transactions on Robotics and Automation, 12(5):651-670, October 1996.
- [7] A. Kelly, “Linearized Error Propagation in Odometry,” to appear in International Journal of Robotics Research, 2004.
- [8] E. Krokotov. “Mobile Robot Localization Using a Single Image”. In Proceedings of the IEEE International Conference on Robotics and Automation, volume 2, pages 978-983, 1989.
- [9] R. P. Langley, “The Mathematics of GPS”, GPS World, July 1991, pp 45-50.
- [10] J. J. Leonard, H. F. Durrant-Whyte, "Mobile Robot Localization by Tracking Geometric Beacons." IEEE Transaction on Robotics and Automation Vol. 7, No 3, June 1991.
- [11] L. Matthies, and S. Shafer, “Error Modelling in Stereo Navigation”, IEEE Journal of Robotics and Automation, Vol. RA-3, No. 3, pp 239-248, June 1987.
- [12] R. J. Milliken, and C. J. Zoller, “Principle of Operation of NAVSTAR and System Characteristics”, In Global Positioning System, volume 1, pages 3--14. The Insitute of Navigation, Alexandria, Virginia, USA, 1980.
- [13] K. Sugihara, “Some Location Problems for Robot Navigation Problems Using a Single Camera”, Computer Vision, Graphics, Image Processing, 42(1); 112-129, April 1988.
- [14] R. Talluri and J. K. Aggarwal, "Position Estimation Techniques for an Autonomous Mobile Robot - A Review", in Handbook of Pattern Recognition and Computer Vision, edited by C. H. Chen, L. F. Pau and P.S. P. Wang, 1993, pp. 769-801.
- [15] D. E. Whitney, "The Mathematics of Coordinated Control of Protheses and Manipulators,", J. Dynamic Systems, Measurement, Control, Dec 1972.
- [16] J.E.D. Williams, *From Sails to Satellites*, Oxford University Press, 1994.